

ORIGINAL ARTICLE

Asymmetric anionic polymerizations of *N*-substituted itaconimides having chiral amino-acid esters

Kazuhiro Yamabuki, Fumiko Hashino, Motohisa Azechi, Kenjiro Onimura and Tsutomu Oishi

Chiral itaconimides bearing the amino-acid methyl ester (MRII), such as phenylglycine-, phenylalanine- and leucine-methyl ester, at the side chain (*S*)- or (*R*)-MPGII, (*S*)-MPAII and (*S*)-MLII, respectively, were successfully synthesized and then polymerized with organometal–chiral ligand complexes such as *n*-butyllithium/(–)-sparteine [*n*-BuLi/(–)-Sp], *n*-BuLi/(*S,S*)-(1-ethylpropylidene)bis(4-benzyl-2-oxazoline) [*n*-BuLi/(*S,S*)-Bnbox], Et₂Zn-(–)-Sp and Et₂Zn-(*S,S*)-Bnbox in toluene or tetrahydrofuran (THF) to obtain optically active polymers. The effects of polymerization conditions on optical activity and the structure of poly(MRII)s were investigated by gel permeation chromatography (GPC), circular dichroism, specific rotation and ¹³C nuclear magnetic resonance measurements. The yields of methanol-insoluble part of the polymer and the *M_n*s, as well as the chiroptical properties of poly(MRII)s, were strongly affected by organometals, ligands, solvents and temperature. The behaviors of poly(MRII)s were different according to *N*-substituents. In addition, the polymers obtained with *n*-BuLi as the anionic initiator had higher stereoregularity than those obtained with a radical initiator.

Polymer Journal (2011) 43, 516–524; doi:10.1038/pj.2011.17; published online 6 April 2011

Keywords: amino-acid ester; anionic polymerization; asymmetric polymerization; itaconimide

INTRODUCTION

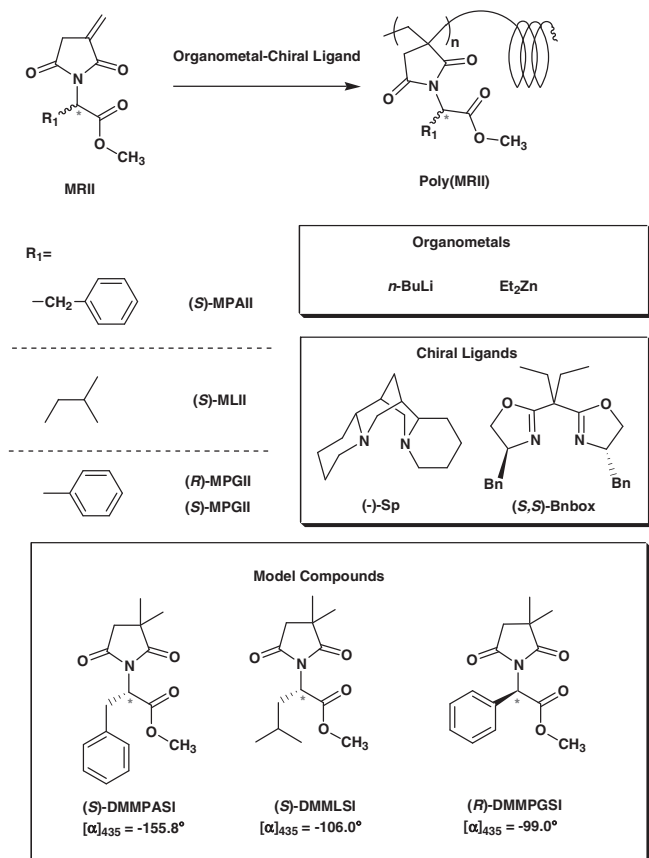
Chiral synthetic polymers are particularly interesting because of their applications as chiral stationary phases for high-performance liquid chromatography, chiral catalysts and chiral reagents. Moreover, for the function of biopolymers such as deoxyribonucleic acid (DNA) and protein, it is important to control secondary structures such as helices. Syntheses of helical polymers, such as poly(alkyl methacrylate)s,^{1–3} polyacetylenes,^{4–7} polyisocyanates⁸ and polyisocyanides,^{9–11} have been reported by several researchers. Physical and steric interactions between side chains are essential factors in the formation of the helical structures of these polymers. For example, Okamoto *et al.*^{1–3} reported that polymerization of triphenylmethyl methacrylate with organolithium/chiral ligand complexes successfully proceeded to yield a polymer with a single-handed helical structure formed by steric repulsion between the bulky side chains. Masuda *et al.*^{12–15} successfully synthesized poly(*N*-propargylamide)s with a well-controlled helical structure based on hydrogen bonding between the chiral side chains, as well as steric repulsion.

We systematically investigated the asymmetric polymerization of *N*-substituted maleimides (RMIs) and reported properties of the resulting polymer with chiral recognition ability. In recent years, our research focus has been on the asymmetric polymerization of RMIs bearing amino-acid derivative moieties, and we have reported the higher-order structure of polymers induced by hydrogen bonding between the amino-acid side chains.^{16–23}

An *N*-substituted itaconimide (RII) is a five-membered ring compound and RMI, but RII is different from RMI in the position of the double bond; that is, RII is a 1,1-disubstituted ethylene.^{24,25} Therefore, it is hoped that the polymers obtained from asymmetric polymerization of RII have conformational chirality based on the structure of the main chain and bulky methacrylate reported previously.^{1–3} However, reports on the asymmetric polymerizations of RII are infrequent.

Previously, we reported asymmetric anionic polymerizations of achiral RIIs, such as *n*-diphenylmethylytaconimide, and radical and anionic polymerizations of chiral RIIs bearing a methylbenzyl group and a cholesterol group.^{26–28} However, asymmetric anionic polymerization of a chiral RII-bearing amino acid has not been reported yet. These poly(RII)s are possible novel chiral materials.

In this study, we report for the first time the syntheses of new optically active polymers consisting of itaconimides bearing chiral amino-acid methyl esters on side chains (MRII), which are phenylglycine-, phenylalanine- and leucine-methyl esters (MPGII, MPAII and MLII, respectively), by anionic polymerization with only organometals or organometal–chiral ligand complexes (Scheme 1). To understand the effect of bulky *N*-substituents and interaction between the side chains on the polymerization abilities and chiroptical properties of the obtained polymers, gel permeation chromatography (GPC), circular dichroism (CD) spectroscopy, optical rotation and ¹³C nuclear magnetic resonance (NMR) measurements were used.



Scheme 1 Asymmetric anionic polymerization of chiral MRIIs having amino-acid methyl esters.

EXPERIMENTAL PROCEDURE

Measurements

Hg-line-specific rotations were measured with a Jasco P-1030 spectrophotometer (Japan Spectroscopic, Tokyo, Japan) at 25 °C (quartz cell length (l)=10 cm; concentration (c), 0.1–1.0 g dl⁻¹ in tetrahydrofuran, THF). CD spectra were measured in THF with a Jasco J-805 (Japan Spectroscopic; quartz cell l =0.1 cm; c =0.01–0.1 g dl⁻¹ in THF). Ultraviolet (UV) spectra were obtained by measurements in THF with Shimadzu UV-2200 (Shimadzu, Kyoto, Japan). The number-average-molecular weights (M_n 's) of the polymers were measured with GPC using THF at 50 °C and with polystyrene as the standard, with an LC-10AS instrument (Shimadzu) equipped with a UV-visible photo spectrometer SPD-10A (Shimadzu) and a polarimetric detector OR-990 (Japan Spectroscopic). ¹H and ¹³C NMR spectra of polymers were measured in chloroform-*d* at room temperature in the presence of tetramethylsilane (TMS) as an internal standard with a JEOL EX-270 (JEOL Ltd., Tokyo, Japan; ¹H, 270 MHz; ¹³C, 68.7 MHz) spectrometer.

Syntheses of monomer (MRII)

Synthesis of (R)-N-[α -(methoxycarbonyl)phenylmethyl]itaconamic acid. D-2-Phenylglycine methyl ester ((R)-phenylglycine methyl ester) was synthesized from D-2-phenylglycine [(R)-(-)- α -aminophenylacetic acid] by a previously described method.¹⁶ A solution of itaconic anhydride (5.6 g, 50 mmol) in ethyl acetate (50 ml) was added dropwise to a solution of D-2-phenylglycine methyl ester (8.3 g, 50 mmol) in ethyl acetate (100 ml) at room temperature, and the mixture was stirred overnight. The reaction mixture was washed with water and saturated brine and then dried over Na₂SO₄. After filtration, the solvent was removed by evaporation to yield (R)-N-[α -(methoxycarbonyl)phenylmethyl]itaconamic acid ((R)-MPGIA) as a white powder (13.5 g, 98.0%, m.p.: 92–94 °C).

¹H NMR (δ in p.p.m. from TMS in CDCl₃): 7.45–7.23 (m, 5H, phenyl), 7.10–6.90 (bs, 1H, CONH), 6.49 and 5.86 (s, 2H, CH₂=C), 5.53–5.69 (q, 1H, N-CH), 3.75 (s, 3H, CH₃), 3.31 (m, 2H, C=C-CH₂).

Synthesis of (R)-N-[α -(methoxycarbonyl)phenylmethyl]itaconimide. (R)-MPGIA (12.5 g, 45 mmol) in dry benzene (100 ml) was stirred at 50 °C to dissolve it; further, ZnCl₂ (7.5 g, 45 mmol) was added all at once. The mixture was heated at 80 °C. 1,1,1,3,3,3-Hexamethyldisilazane (23.2 ml, 90 mmol) in dry benzene (50 ml) was added dropwise to the suspension with stirring. The reaction mixture was refluxed for 2.5 h. The reaction mixture was cooled to room temperature, then filtrated and concentrated under reduced pressure and dissolved ethyl acetate (100 ml). This solution was washed with 0.1 N aqueous hydrochloric acid, saturated aqueous sodium hydrogen carbonate and saturated brine and then dried over Na₂SO₄. After filtration, the organic solution was concentrated under reduced pressure to afford crude (R)-N-[α -(methoxycarbonyl)phenylmethyl]itaconimide ((R)-MPGII). The crude (R)-MPGII was purified by column chromatography (silicagel, *n*-hexane/ethyl acetate=1:1) to obtain pure (R)-MPGII as a yellow oil (4.7 g, 40.3%, [α]₄₃₅=+127.4° (c =1.0 g dl⁻¹, l =10 cm, THF)).

¹H NMR (δ in p.p.m. from TMS in CDCl₃): 7.45–7.23 (m, 5H, phenyl), 6.40 and 5.92 (s, 2H, CH₂=C), 5.69 (s, 1H, N-CH), 3.85–3.74 (s, 3H, CH₃), 3.36 (s, 2H, C=C-CH₂).

Synthesis of (S)-MPGII. (S)-MPGII was prepared from itaconic anhydride and L-2-phenylglycine methyl ester ((S)-phenylglycine methyl ester), according to a reaction similar to that for (R)-MPGII (47.0%, yellow oil, [α]₄₃₅=-126.2° (c =1.0 g dl⁻¹, l =10 cm, THF)).

¹H NMR (δ in p.p.m. from TMS in CDCl₃): 7.45–7.23 (m, 5H, phenyl), 6.40 and 5.92 (s, 2H, CH₂=C), 5.69 (s, 1H, N-CH), 3.85–3.74 (s, 3H, CH₃), 3.36 (s, 2H, C=C-CH₂).

Synthesis of (S)-N-[α -(methoxycarbonyl)phenylethyl]itaconimide. (S)-MPAIA was prepared from itaconic anhydride and (S)-phenylalanine methyl ester, according to a method similar to that for (R)-MPGIA. (S)-N-[α -(methoxycarbonyl)phenylethyl]itaconimide ((S)-MPAII) was synthesized from (S)-MPAIA, ZnBr₂ and 1,1,1,3,3,3-hexamethyldisilazane, according to a method similar to that for (R)-MPGII. The reaction mixture was refluxed for 2.5 h. The crude (S)-MPAII was purified by column chromatography (silicagel, *n*-hexane/ethyl acetate=4:1) to obtain pure (S)-MPAII as a yellow oil (32.5%, [α]₄₃₅=-404.8° (c =1.0 g dl⁻¹, l =10 cm, THF)).

¹H NMR (δ in p.p.m. from TMS in CDCl₃): 7.25–7.18 (m, 5H, phenyl), 6.26 and 5.55 (t, 2H, CH₂=C), 5.11–5.05 (q, 1H, N-CH), 3.77 (s, 3H, CH₃), 3.54–3.38 (t, 2H, C=C-CH₂), 3.19–3.15 (t, 2H, N-C-CH₂).

Synthesis of (S)-N-[α -(methoxycarbonyl)-3-methylbutyl]itaconimide. (S)-MLIA was prepared from itaconic anhydride and (S)-leucine methyl ester according to a method similar to that for (R)-MPGIA. (S)-N-[α -(methoxycarbonyl)-3-methylbutyl]itaconimide ((S)-MLII) was synthesized from (S)-MLIA, ZnBr₂ and 1,1,1,3,3,3-hexamethyldisilazane according to a method similar to that for (R)-MPGII. The reaction mixture was refluxed for 4 h. The crude (S)-MLII was purified by column chromatography (silicagel, *n*-hexane/ethyl acetate=4:1) to obtain pure (S)-MLII as a yellow oil (45.4%, [α]₄₃₅=-344.3° (c =1.0 g dl⁻¹, l =10 cm, THF)).

¹H NMR (δ in p.p.m. from TMS in CDCl₃): 6.38 and 5.67 (t, 2H, CH₂=C), 4.92–4.81 (q, 1H, N-CH), 3.71 (s, 3H, -O-CH₃), 3.36 (t, 2H, C=C-CH₂), 2.35–2.24, 1.99–1.86 (q, 2H, CH-CH₂), 1.33–1.51, (m, 1H, CH-(CH₃)₂), 0.94–0.84 (dd, 6H, CH₂-(CH₃)₂).

Syntheses of the model compounds (DMMRSI)

Synthesis of (S)-N-[α -(methoxycarbonyl)-3-methylbutyl- α,α -dimethylsuccinimide. 2,2-Dimethylsuccinic acid (1.0 g, 6.8 mmol) in 10-ml acetyl chloride was refluxed for 4 h and then concentrated under reduced pressure. The obtained 2,2-dimethylsuccinic acid anhydride (0.4 g, 3.1 mmol) in acetyl chloride was refluxed for 4 h, then concentrated under reduced pressure and neutralized by saturated aqueous sodium hydrogen carbonate. The organic layer was extracted by ethyl acetate (three times) and washed with saturated brine. The solution was dried over Na₂SO₄. After filtration, the organic solution was concentrated under reduced pressure to afford crude (S)-N-[α -(methoxycarbonyl)-3-methylbutyl- α,α -

α -dimethylsuccinimide ((*S*)-DMMLSI). The crude (*S*)-DMMLSI was purified by column chromatography (silicagel, *n*-hexane/ethyl acetate=1:1) to obtain pure (*S*)-DMMLSI as a white oil (0.2 g, 7.5%, $[\alpha]_{435}=-106.0^\circ$ ($c=1.0$ g dl⁻¹, $l=10$ cm, THF)).

¹H NMR (δ in p.p.m. from TMS in CDCl₃): 4.75–4.83 (q, 1H, N-CH), 3.74 (s, 3H, CH₃), 2.59 (t, 2H, C=C-CH₂), 2.30–2.14, 1.96–1.80 (q, 2H, CH-CH₂), 1.25–1.45, (m, 1H, CH-(CH₃)₂), 1.38 (dd, 6H, C-(CH₃)₂), 0.98–0.84 (d, 6H, CH₂-(CH₃)₂).

Synthesis of (*S*)-*N*-[α -(methoxycarbonyl)phenylethyl]- α,α -dimethylsuccinimide. (*S*)-*N*-[α -(methoxycarbonyl)phenylethyl]- α,α -dimethylsuccinimide ((*S*)-DMMPASI) was prepared from 2,2-dimethylsuccinic acid and (*S*)-phenylalanine methyl ester according to a method similar to that for (*S*)-DMMLSI. The crude (*S*)-DMMPASI was purified by column chromatography (silicagel, *n*-hexane/dichloromethane=2:1) to obtain pure (*S*)-DMMPASI as a white solid (24.7%, $[\alpha]_{435}=-155.8^\circ$ ($c=1.0$ g dl⁻¹, $l=10$ cm, THF)).

¹H NMR (δ in p.p.m. from TMS in CDCl₃): 7.25–7.18 (m, 5H, phenyl), 5.04–4.97 (q, 1H, N-CH), 3.78 (s, 3H, CH₃), 3.51–3.44 (t, 1H, C=C-CH₂), 2.35–2.34 (t, 2H, CH-CH₂), 1.15–1.00 (d, 6H, C-(CH₃)₂).

Synthesis of (*S*)-*N*-[α -(methoxycarbonyl)phenylmethyl]- α,α -dimethylsuccinimide. (*S*)-*N*-[α -(methoxycarbonyl)phenylmethyl]- α,α -dimethylsuccinimide ((*R*)-DMMPGSI) was prepared from 2,2-dimethylsuccinic acid and (*R*)-phenylglycine methyl ester, according to a method similar to that for (*S*)-DMMLSI. The crude (*R*)-DMMPGSI was purified by column chromatography (silicagel, dichloromethane) to obtain pure (*R*)-DMMPGSI as a white oil (9.0%, $[\alpha]_{435}=-99.0^\circ$ ($c=1.0$ g dl⁻¹, $l=10$ cm, THF)).

¹H NMR (δ in p.p.m. from TMS in CDCl₃): 7.60–7.32 (m, 5H, phenyl), 6.82 (s, 1H, N-CH), 3.84 (s, 3H, CH₃), 2.44 (s, 1H, C=C-CH₂), 1.40 (d, 6H, C-(CH₃)₂).

Chiral ligands

Commercially available (–)-sparteine (Sp) was purified by distillation under reduced pressure ($[\alpha]_{435}=-10.3^\circ$ ($c=1.0$ g dl⁻¹, $l=10$ cm, THF)).

(4*S*)-2,2'-(1-ethylpropylidene)bis[4-(1-phenylethyl)]-4,5-dihydrooxazole ((*S*)-Bnbox) was prepared from (*S*)-phenylalaninol and diethylmalonyl dichloride, according to a previously published method ($[\alpha]_{435}=-128.0^\circ$ ($c=1.0$ g dl⁻¹, $l=10$ cm, THF)).¹⁶

¹H NMR (δ in p.p.m. from TMS in CDCl₃): 7.31–7.18 (m, 10H, phenyl), 4.46–4.35 (m, 2H, N-CH), 4.14 (t, 2H, CH₂-phenyl), 3.97 (dd, 2H, CH₂-phenyl), 3.14, 2.65 (dd, 4H, CH₂-O-), 1.98 (q, 4H, CH₂-), 0.83 (t, 6H, CH₃).

Reagents and solvents

Solvents used for syntheses, polymerizations and measurements were purified in the usual manner. Commercially available *n*-butyllithium (*n*-BuLi)/*n*-hexane (1.55 mol l⁻¹) and diethylzinc/*n*-hexane (1.55 mol l⁻¹) solutions were used without purification.

Anionic polymerization

Monomers (0.5 g) and chiral ligands were placed in a schlenk reaction tube (50 ml) and a pear-shaped flask (10 ml), respectively. They were evacuated by a vacuum pump and then replaced by dry nitrogen gas. The polymerization solvent was directly added to a ligand solution by using a syringe under a nitrogen atmosphere. An organometal solution was added to a ligand solution by using a syringe and then the mixed solution was added into the monomer solution maintained at polymerization temperature, using a cannula under a nitrogen atmosphere. Polymerization was terminated with a small amount of methanol containing one drop of 6 N aqueous hydrochloric acid. The reaction mixture was poured into excess methanol to precipitate the polymers. Purification of the polymer was performed with reprecipitation from a THF–MeOH system three times and dried *in vacuo* at 25 °C for 2 days.

Radical polymerization

Radical polymerization was performed with α,α' -azoisobutyronitrile (AIBN) as the initiator in toluene or THF, in a sealed tube at 60 °C under a nitrogen atmosphere. After polymerization, the solution was poured into a large amount of methanol to precipitate the polymer. The resulting polymer was purified by reprecipitation from a THF–MeOH system two times and dried *in vacuo* at 25 °C for 2 days.

RESULTS AND DISCUSSION

Polymerizations of MRIIs

To investigate the relationship between bulky *N*-substituents and polymerization abilities, MRIIs were polymerized in various conditions.

Tables 1 and 2 show the results of asymmetric anionic polymerizations with organometal–chiral ligand complexes, such as *n*-butyllithium/(–)-sparteine [*n*-BuLi/(–)-Sp], *n*-BuLi/(*S,S*)-(1-ethylpropylidene)bis(4-benzyl-2-oxazoline) [*n*-BuLi/(*S,S*)-Bnbox], Et₂Zn(–)-Sp and Et₂Zn-(*S,S*)-Bnbox, and radical polymerizations with AIBN of (*R*)-MPGII and (*S*)-MPGII. Tables 3 and 4 show the results of anionic and radical polymerizations of (*S*)-MPAII and (*S*)-MLII, respectively. All anionic polymerizations proceeded in a homogeneous system. However, in the radical polymerization, the precipitation occurred during the reaction.

Polymerizations of (*R*)- and (*S*)-MPGII. The yields of the methanol-insoluble part and the M_n s of poly((*R*)- or (*S*)-MPGII)s were strongly affected by organometals, ligands, solvents and temperature. The polymerization using only *n*-BuLi (run 1 in Table 1) afforded the highest molecular weight ($M_n=2600$), whereas the polymerization with *n*-BuLi/(–)-Sp in toluene at 0 °C (run 3 in Table 1) afforded a higher yield (55.2%). These results indicate that the catalytic activity

Table 1 Anionic and radical polymerizations of (*R*)-MPGII^a

Run	Initiator ^b	Solv.(ml)	Temp (°C)	Time (h)	Yield ^c (%)	$M_n^d \times 10^{-3}$	M_w/M_n^d	$[\alpha]_{435}^e$
1	<i>n</i> -BuLi	Tol. (4)	0	24	46.9	2.6	1.38	–1.4
2	<i>n</i> -BuLi/(–)-Sp	Tol. (4)	r.t.	24	15.8	1.8	1.19	+4.0
3	<i>n</i> -BuLi/(–)-Sp	Tol. (4)	0	24	55.2	2.1	1.04	–0.3
4	<i>n</i> -BuLi/(–)-Sp	Tol. (4)	–40	72	15.7	1.7	1.09	+13.2
5	<i>n</i> -BuLi/(<i>S,S</i>)-Bnbox	Tol. (4)	r.t.	24	16.4	1.8	1.07	+5.4
6	<i>n</i> -BuLi/(<i>S,S</i>)-Bnbox	Tol. (4)	0	24	22.1	2.0	1.04	–4.0
7	<i>n</i> -BuLi/(<i>S,S</i>)-Bnbox	Tol. (4)	–40	72	2.7	1.9	1.07	–4.7
8	<i>n</i> -BuLi/(<i>S,S</i>)-Bnbox	THF (3)	0	24	12.5	2.3	1.16	–2.5
9	AIBN ^f	Tol. (3)	60	24	65.5	10.2, 1.8	2.5, 1.3	–18.0

Abbreviations: r.t., room temperature; THF, tetrahydrofuran; Tol., toluene.

^a0.5 g.

^b(Initiator)/(monomer)=0.1.

^cMethanol-insoluble part.

^dBy gel permeation chromatography (THF).

^e $c=1.0$ g dl⁻¹, $l=10$ cm (in THF).

^f2,2'-Azobisisobutyronitrile.

of only *n*-BuLi is lower than that of *n*-BuLi/(–)-Sp: associating *n*-BuLi in nonpolar solvent (toluene) had reduced anion species. In contrast, the yield and the molecular weight of radical polymerization with AIBN (run 9 in Table 1) were higher than those of all anionic

polymerizations (65.5%, $M_n=10\,200$). In addition, in the case of anionic polymerizations of (S)-MPGII, the polymerization with *n*-BuLi/(–)-Sp in toluene (runs 1 and 2 in Table 2) afforded lower M_n than (R)-MPGII (runs 6 and 7 in Table 1).

Table 2 Anionic polymerizations of (S)-MPGII^a

Run	Initiator ^b	Solv. (ml)	Temp (°C)	Time (h)	Yield ^c (%)	M_n^d (%)	$M_w/M_n^d \times 10^{-3}$	$[\alpha]_{435}^e$
1	<i>n</i> -BuLi/(S,S)-Bnbox	Tol. (3)	0	24	13.6	1.2	1.15	–3.0
2	<i>n</i> -BuLi/(S,S)-Bnbox	Tol. (3)	–40	24	20.8	1.1	1.15	–38.5

Abbreviations: THF, tetrahydrofuran; Tol., toluene.

^a0.5 g.

^b(Initiator)/(monomer)=0.1.

^cMethanol-insoluble part.

^dBy gel permeation chromatography (THF).

^e $c=1.0\text{ g dl}^{-1}$, $l=10\text{ cm}$ (in THF).

Polymerizations of (S)-MPAII

The polymerization using only *n*-BuLi (run 1 in Table 3) afforded higher molecular weight ($M_n=2400$) as in the polymerization of (R)-MPGII. In anionic polymerizations with *n*-BuLi and *n*-BuLi/ligand complex as the initiator, the yields of the methanol-insoluble part of polymers obtained in THF decreased compared with those obtained in toluene. This finding may be attributed to the coordination between the oxygen of THF and *n*-BuLi (or *n*-BuLi/ligand complex) to form a bulkier complex. However, the yield and the molecular weight of radical polymerization with AIBN (run 9 in Table 3) were also higher than those of all anionic polymerizations (45.9%, $M_n=7300$).

Table 3 Anionic and radical polymerizations of (S)-MPAII^a

Run	Initiator ^b	Solv. (ml)	Temp. (°C)	Time (h)	Yield ^c (%)	$M_n^d \times 10^{-3}$	M_w/M_n^d	$[\alpha]_{435}^e$ (deg)
1	<i>n</i> -BuLi	Tol. (5)	0	24	24.8	2.4	1.20	–203.7 ^f
2	<i>n</i> -BuLi	THF (5)	0	24	6.0	1.8	1.20	–280.3 ^f
3	<i>n</i> -BuLi/(–)-Sp(1/1.2)	Tol. (4)	0	24	35.7	1.2	1.18	–195.1
4	<i>n</i> -BuLi/(–)-Sp(1/1.2)	Tol. (4)	–78	24	24.8	2.6	1.14	–181.4
5	<i>n</i> -BuLi/(–)-Sp(1/1.2)	THF (4)	0	24	6.3	2.1	1.1	–232.8
6	<i>n</i> -BuLi/(S,S)-Bnbox(1/1.2)	Tol. (4)	0	24	24.3	1.2	1.17	–185.3
7	<i>n</i> -BuLi/(S,S)-Bnbox(1/1.2)	Tol. (4)	–40	24	Trace (59.2)	(0.6)	(1.07)	(–156.8)
8	<i>n</i> -BuLi/(S,S)-Bnbox(1/1.2)	Tol. (5)	–78	24	Trace	—	—	—
9	AIBN ^g	Tol. (2)	60	24	45.9	7.3	2.7	–202.2

Abbreviations: THF, tetrahydrofuran; Tol., toluene.

^a0.5 g.

^bOrganometal/(monomer)=0.1, (AIBN)/(monomer)=0.1.

^cMethanol-insoluble part(hexane-insoluble part).

^dBy gel permeation chromatography (THF).

^e $c=1.0\text{ g dl}^{-1}$, $l=10\text{ cm}$ (in THF).

^f $c=0.1\text{ g dl}^{-1}$, $l=10\text{ cm}$ (in THF).

^g2,2'-Azobisisobutyronitrile.

Table 4 Anionic and radical polymerizations of (S)-MLII^a

Run	Initiator ^b	Solv. (ml)	Temp. (°C)	Time (h)	Yield ^c (%)	$M_n^d \times 10^{-3}$	M_w/M_n^d	$[\alpha]_{435}^e$ (deg)
1	<i>n</i> -BuLi	Tol. (3)	0	24	46.2	1.4	1.23	–92.3
2	<i>n</i> -BuLi/(–)-Sp	Tol. (3)	0	24	91.0	1.7	1.36	–69.1
3	<i>n</i> -BuLi/(–)-Sp	Tol. (3)	–40	72	82.5	1.7	1.23	–76.7
4	<i>n</i> -BuLi/(–)-Sp	Tol. (3)	–78	72	81.7	2.2	1.21	–90.7
5	<i>n</i> -BuLi/(S,S)-Bnbox	Tol. (3)	0	24	69.4	1.7, 0.8	1.1, 1.0	–91.8
6	<i>n</i> -BuLi/(S,S)-Bnbox	Tol. (3)	–40	72	77.2	1.8, 0.7	1.1, 1.1	–107.3
7	<i>n</i> -BuLi/(S,S)-Bnbox	Tol. (3)	–78	72	56.0	2.2, 1.0	1.1, 1.0	–93.4
8	<i>n</i> -BuLi/(S,S)-Bnbox	THF (3)	0	24	79.3	2.0, 0.8	1.1, 1.0	–98.1
9	Et ₂ Zn/(–)-Sp	Tol. (3)	–40	72	48.2	2.6, 0.6	1.4, 1.1	–103.2
10	Et ₂ Zn/(–)-Sp	Tol. (3)	–78	72	39.1	1.8, 0.7	1.1, 1.1	–109.1 ^f
11	Et ₂ Zn/(–)-Sp	THF (3)	–78	72	43.5	2.5, 0.7	1.1, 1.1	–136.8
12	Et ₂ Zn/(S,S)-Bnbox	Tol. (3)	–40	72	42.4	1.6, 0.7	1.1, 1.1	–88.5 ^f
13	AIBN ^g	Tol. (3)	60	24	82.4	74.1	4.2	–128.8
14	AIBN ^g	THF (3)	60	24	46.2	5.9	1.3	–130.2

Abbreviations: THF, tetrahydrofuran; Tol., toluene.

^a0.5 g.

^b(Organometal)/(monomer)=0.1.

^cHexane-insoluble part.

^dBy gel permeation chromatography (THF).

^e $c=1.0\text{ g dl}^{-1}$, $l=10\text{ cm}$ (in THF).

^f $c=0.5\text{ g dl}^{-1}$, $l=10\text{ cm}$ (in THF).

^g2,2'-Azobisisobutyronitrile.

Polymerizations of (S)-MLII. Unlike polymerizations of (R)-MPGII and (S)-MPAII, the polymer obtained with *n*-BuLi had lower molecular weight ($M_n=1400$) and yield (46.2%) than those of polymers obtained with organometal–chiral ligand complexes (for example, run 4 in Table 4; 81.7%, $M_n=2200$). Moreover, the radical polymerization with AIBN in toluene (run 13 in Table 4) afforded a much higher yield and molecular weight (82.4%, $M_n=74\,100$). These results show that bulky organometal–chiral ligand complexes and exo-methylene moiety of MLII formed more stable anion species because of the decreasing bulkiness of the *N*-substituent. These results were consistent with results of anionic polymerizations of *N*-substituted maleimides bearing the same amino-acid methyl ester (D-phenylglycine methyl ester and L-leucin methyl ester).^{22,29}

Polymerization Abilities of MRIs. On the basis of the above results of polymerizations of MRII, the higher polymerization ability of (R)-MPGII was observed in only the *n*-BuLi system. However, in the organometal/chiral ligand complex system, (S)-MLII showed high polymerization ability. These results suggest that the steric hindrance between anionic initiators and *N*-substituents is involved in the anionic polymerization of MRII. In radical polymerization, the polymerization ability of MRII increased in the following order: MPAII < MPGII < MLII. This result may be due to the bulkiness of *N*-substituted groups and interactions between the side chains and initiators.

In previous studies, many researchers have reported polymerizations of exo-methylene monomers except for itaconimide. For example, Ueda *et al.*³⁰ reported radical and anionic polymerizations of α -methyleneindane (MI), which is a cyclic analog of α -methylene-styrene. Stille and group³¹ also reported radical, anionic and group-transfer polymerization of α -methylene- γ -methylene- γ -butyrolactone. In addition, the radical polymerization of 5-methylene-2,2-dimethyl-1,3-dioxolan-4-one and the anionic polymerization of methyl bicyclobutane-1-carboxylate were reported by Endo's group and Kitayama's group, respectively.^{32,33} In recent years, Nakano *et al.*^{34–37} has reported radical, anionic and cationic polymerizations of 2,7-di-*n*-pentylidibenzofulvene and dibenzofulvene, which are 1,1-diphenylethylene analogs and yield π -stacked polymers.

For the polymerization of MI, the radical polymerization with AIBN produced a lower yield and a lower molecular weight of poly(MI) compared with those of poly(MRII).³⁰ This finding indicates that MI has a bigger effect on the steric hindrance in the transition state of propagation compared with MRII or side reactions, such as chain transfer reactions and disproportional reactions. In contrast, the anionic polymerization of MI with *n*-BuLi (in THF at 20 °C) provided a higher yield and higher molecular weight (96.4%, $M_n=18\,200$) than the yield and molecular weight of MRII (in toluene at 0 °C). As a result of the anionic polymerizations, MI with electron-rich double bonds had a higher polymerization ability than MRII with electron-poor double bonds. This finding may be attributed to interactions between lithium ions and carbonyl groups of the succinimide and amino-acid moiety in MRII or differences in polymerization conditions, such as the anionic polymerization of the MI run in a polar solvent (THF) at a high concentration (3.85 mol l⁻¹) at a high temperature (20 °C).

Chiroptical properties of Poly(MRII)

To investigate the effect of a chiral *N*-substituent and an achiral/chiral initiator on the structures of poly(MRIs), specific optical rotations and CD spectra of poly(MRIs) were measured. In addition, the specific optical rotations of polymers were compared with those of

each model compound to understand the main chain structures of polymers obtained by anionic polymerization. The structures of the model compounds are shown in Scheme 1.

Chiroptical properties of Poly[(R)-MPGII] and Poly[(S)-MPGII]. Tables 1 and 2 show specific optical rotations of poly[(R)-MPGII]s (monomer (R)-MPGII; $[\alpha]_{435}=+127.4^\circ$) and poly[(S)-MPGII]s (monomer (S)-MPGII; $[\alpha]_{435}=-126.2^\circ$), respectively. On the basis of the specific optical rotation of the model compound (R)-DMMPGSI ($[\alpha]_{435}=-99.0^\circ$), all rotations of poly[(R)-MPGII]s obtained by the anionic polymerization shifted in the positive direction even in the absence of chiral ligands ($[\alpha]_{435}=-18.0^\circ$ to $+13.2^\circ$). These results indicate that poly[(R)-MPGII]s

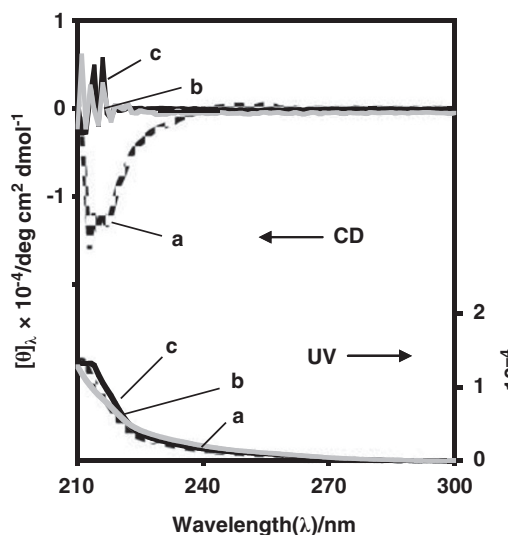


Figure 1 Circular dichroism (CD) and ultraviolet (UV) spectra of (a) (R)-DMMPGSI and (b) poly((R)-MPGII) obtained with *n*-BuLi/(S,S)-Bnbox in Tol. at r.t. ($[\alpha]_{435}=+5.4^\circ$; run 5 in Table 1), and (c) poly((R)-MPGII) obtained with *n*-BuLi/(S,S)-Bnbox in Tol. at 0 °C ($[\alpha]_{435}=-4.0^\circ$; run 6 in Table 1).

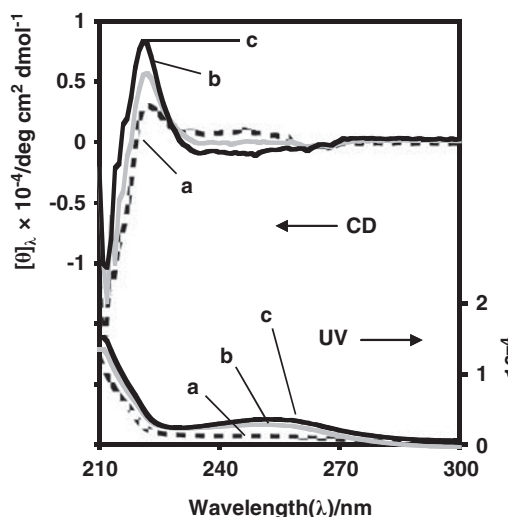


Figure 2 Circular dichroism (CD) and ultraviolet (UV) spectra of (a) (S)-DMMPASI and (b) poly((S)-MPAII) obtained with *n*-BuLi in Tol. at 0 °C ($[\alpha]_{435}=-203.7^\circ$; run 1 in Table 3) and (c) poly((S)-MPAII) obtained with *n*-BuLi/(S,S)-Bnbox in Tol. at 0 °C ($[\alpha]_{435}=-185.3^\circ$; run 6 in Table 3).

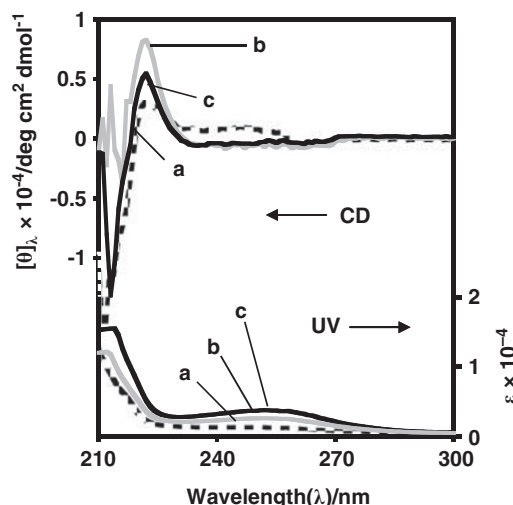


Figure 3 Circular dichroism (CD) and ultraviolet (UV) spectra of (a) (S)-DMMPASI and (b) poly((S)-MPAII) obtained with *n*-BuLi/(–)-Sp in Tol. at 0 °C ($[\alpha]_{435} = -195.1^\circ$; run 3 in Table 3), and (c) poly((S)-MPAII) obtained with *n*-BuLi/(–)-Sp in THF at 0 °C ($[\alpha]_{435} = -232.8^\circ$; run 5 in Table 3).

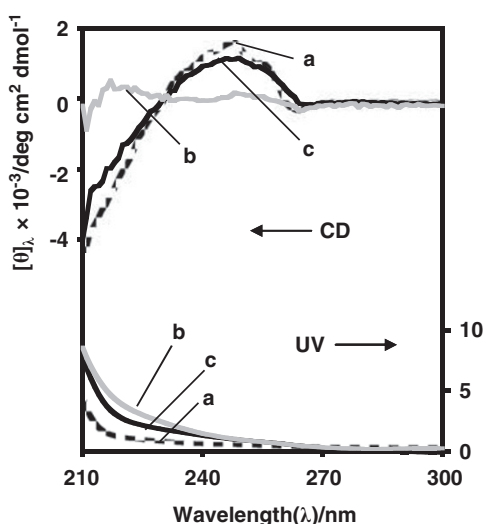


Figure 4 Circular dichroism (CD) and ultraviolet (UV) spectra of (a) (S)-DMMLSI and (b) poly((S)-MLII) obtained with *n*-BuLi/(–)-Sp in Tol. at 0 °C ($[\alpha]_{435} = -69.1^\circ$; run 2 in Table 4) and (c) poly((R)-MLII) obtained with *n*-BuLi/(S,S)-Bnbox in Tol. at 0 °C ($[\alpha]_{435} = -91.8^\circ$; run 5 in Table 4).

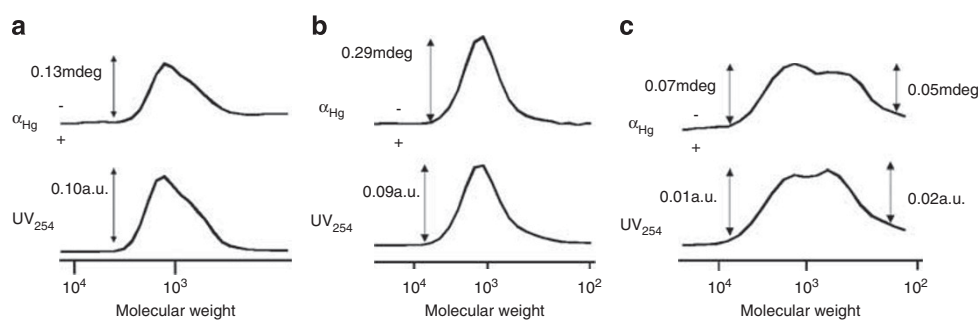


Figure 5 Gel permeation chromatography curves for (a) poly((S)-MPGII) initiated by *n*-BuLi/(S,S)-Bnbox at -40°C in Tol. ($[\alpha]_{435} = -38.5^\circ$; run 2 in Table 2), (b) poly((S)-MPAII) initiated by *n*-BuLi/(S,S)-Bnbox in Tol. at 0 °C ($[\alpha]_{435} = -185.3^\circ$; run 6 in Table 3) and (c) poly((S)-MLII) initiated by *n*-BuLi/(S,S)-Bnbox in Tol. at 0 °C ($[\alpha]_{435} = -91.8^\circ$; run 5 in Table 4).

have a structure different from those of (*R*)-DMMPGSI and (*R*)-MPGII, which means that poly[(*R*)-MPGII]s may form higher-order structures in the anionic polymerization system. In addition, the specific rotation of poly[(*R*)- or (*S*)-MPGII] obtained by the anionic polymerization was also affected by organometals, ligands, solvents and temperature, as in the case of the yield and M_n of poly(MPGII). For the polymer obtained with *n*-BuLi/(S,S)-Bnbox in toluene at -40°C , poly[(*S*)-MPGII] ($[\alpha]_{435} = -38.5^\circ$, run 2 in Table 2) showed a bigger change of specific optical rotation toward the corresponding model compound than poly[(*R*)-MPGII] ($[\alpha]_{435} = -4.7^\circ$, run 7 in Table 1). There are possibly different interaction strengths between an organometal–chiral ligand complex (*n*-BuLi/(S,S)-Bnbox) and optical isomers ((*S*)-MPGII and (*R*)-MPGII). Thus, (*S*)-MPGII was better able to approach the growing chain end in a single direction to avoid stereorepulsion between the *n*-BuLi/(S,S)-Bnbox complex and the monomer.

Figure 1 shows CD and UV spectra of poly(*R*)-MPGII (runs 5 and 6 in Table 1) and the model compound (*R*)-DMMPGSI. Although a large negative Cotton effect of the model compound was observed at ~ 220 nm, which was mainly attributable to the $n\text{-}\pi^*$ electron transition due to carbonyl groups in the *N*-substituent and itaconimide moiety, a small positive Cotton effect of the polymers was observed in the same region. This result also shows that poly(*R*)-MPGII has a higher-order structure. In spectra of poly(*R*)-MPGII, the polymerization temperature did not have an observed effect on the Cotton effect.

Chiroptical properties of Poly[(S)-MPAII]. Table 3 shows specific optical rotations of poly[(*S*)-MPAII]s (monomer (*S*)-MPAII; $[\alpha]_{435} = -404.8^\circ$). On the basis of the specific optical rotation of the model compound ((*S*)-DMMPASI; $[\alpha]_{435} = -155.8^\circ$), all rotations of poly[(*S*)-MPAII]s shifted in the negative direction ($[\alpha]_{435} = -156.8^\circ$ to -280.3°), meaning poly[(*S*)-MPAII]s may also form higher order structures as do poly[(*R*)-MPGII] and poly[(*S*)-MPGII]. For the anionic polymerization, the specific rotations of polymers obtained in THF were much more shifted to the levorotatory direction than those obtained in toluene. Moreover, for the polymerization in toluene, the specific rotations of polymers obtained with *n*-BuLi/ligand complexes were shifted to the levorotatory direction compared with those obtained with *n*-BuLi and AIBN as initiators. This tendency could be attributed to the difference in structure between the counter metal cations at the propagating chain end.

Figure 2 shows CD and UV spectra of poly[(*S*)-MPAII] (runs 1 and 6 in Table 3) and the model compound (*S*)-DMMPASI. Despite a small peak based on the model compound at ~ 220 nm, larger positive Cotton effects of polymers obtained by the anionic polymerization were observed in the same region. In particular, the polymer obtained

with *n*-BuLi/(*S,S*)-Bnbox showed a larger positive Cotton effect than that of *n*-BuLi. In addition, for the spectra of poly[(*S*)-MPAII] with *n*-BuLi/(–)-Sp, effects of solvents on the Cotton effect were observed (Figure 3). The CD spectrum of poly[(*S*)-MPAII] obtained in toluene showed a larger positive Cotton effect than that obtained in THF under the same polymerization conditions (runs 3 and 5 in Table 3).

These results suggest that anionic polymerizations using *n*-BuLi/ligand complexes in toluene may yield a better-controlled higher-order structure compared with those using only *n*-BuLi. Furthermore, given the intensities of the Cotton effects, it is discernible that the anionic polymerization in toluene is more advantageous for the control of helical structures.

Chiroptical properties of Poly[(*S*)-MLII]. Table 4 shows specific optical rotations of poly[(*R*)-MPGII]s (monomer (*S*)-MLII; $[\alpha]_{435} = -344.3^\circ$). The poly[(*S*)-MLII]s obtained with *n*-BuLi-chiral ligand had negative signs ($[\alpha]_{435} = -69.1^\circ$ to -107.3° , runs 2–8 in Table 4), which showed a larger shift to dextrorotatory direction compared with those of the model compound (*S*)-DMMLSI ($[\alpha]_{435} = -106.0^\circ$) and monomer. In particular, for the *n*-BuLi/ligand complexes series, the specific optical rotations of the polymers obtained with (–)-Sp had the tendency of shifting to dextrorotatory direction relative to polymers obtained with *n*-BuLi/(*S,S*)-Bnbox complexes and polymers obtained by radical polymerization.

Information about chiroptical properties of optically active poly[(*S*)-MLII]s was also obtained by CD and UV spectra. Figure 4 shows CD and UV spectra of poly[(*S*)-MLII] obtained with *n*-BuLi/ligand complexes (runs 2 and 5 in Table 4) and the model compound (*S*)-DMMLSI. Although there was a large positive Cotton effect of the model compound at about 250 nm, a new small positive Cotton effect of the polymer obtained with *n*-BuLi/(–)-Sp ($[\alpha]_{435} = -69.1^\circ$, run 2 in Table 4) was observed at ~ 220 nm. However, the spectrum of the polymer obtained with (*S,S*)-Bnbox ($[\alpha]_{435} = -91.8^\circ$, run 5 in Table 4) showed a spectrum similar to that of the model compound.

The results indicate that (–)-Sp is an appropriate chiral ligand to control the steric structure of poly[(*S*)-MLII] compared with (*S,S*)-Bnbox.

Relationship between M_{ns} of poly(MRII) and optical activities. To investigate the effects of the molecular weights on the optical activities of poly(MPGII), poly(MPAII) and poly(MLII), GPC analysis was performed with UV and polarimetric detectors. Figure 5 represents the GPC curves of poly[(*S*)-MPGII] (run 2 in Table 2), poly[(*S*)-MPAII] (run 6 in Table 3) and poly[(*S*)-MPAII] (run 5 in Table 4).

The curve of poly[(*S*)-MPGII]s obtained with *n*-BuLi/(*S,S*)-Bnbox at -40°C in toluene ($[\alpha]_{435} = -38.5^\circ$) from the polarimetric detector corresponded to that from the UV detector over the range of molecular weights (Figure 5a). Moreover, the curve of poly[(*S*)-MPAII]s obtained with *n*-BuLi/(*S,S*)-Bnbox at 0°C in toluene ($[\alpha]_{435} = -185.3^\circ$) from the polarimetric detector also corresponded to that from the UV detector over the range of molecular weights (Figure 5b). This result indicates that every molecular weight part of the polymers has an equal optical rotation, suggesting that the chiroptical properties were attributable not to terminal chirality but to chiral *N*-substituents and chiral stereogenicity of the whole main chain.

However, the curve of poly[(*S*)-MLII]s obtained with *n*-BuLi/(*S,S*)-Bnbox at 0°C in toluene ($[\alpha]_{435} = -91.8^\circ$) from the UV detector did not fully correspond to that obtained from the polarimetric detector over the range of molecular weights; each intensity ratio of the

bimodal peak was different between the UV detector and the polarimetric detector (Figure 5c). As a result, the optical activity of the polymer with high molecular weight was larger than that of the polymer with low molecular weight; that is, the optical rotation of poly[(*S*)-MLII] was dependent on the molecular weight. This finding suggests the possibility that the polymer with a higher molecular weight forms a higher-order structure, such as a one-handed helix, compared with the polymer with a lower molecular weight.

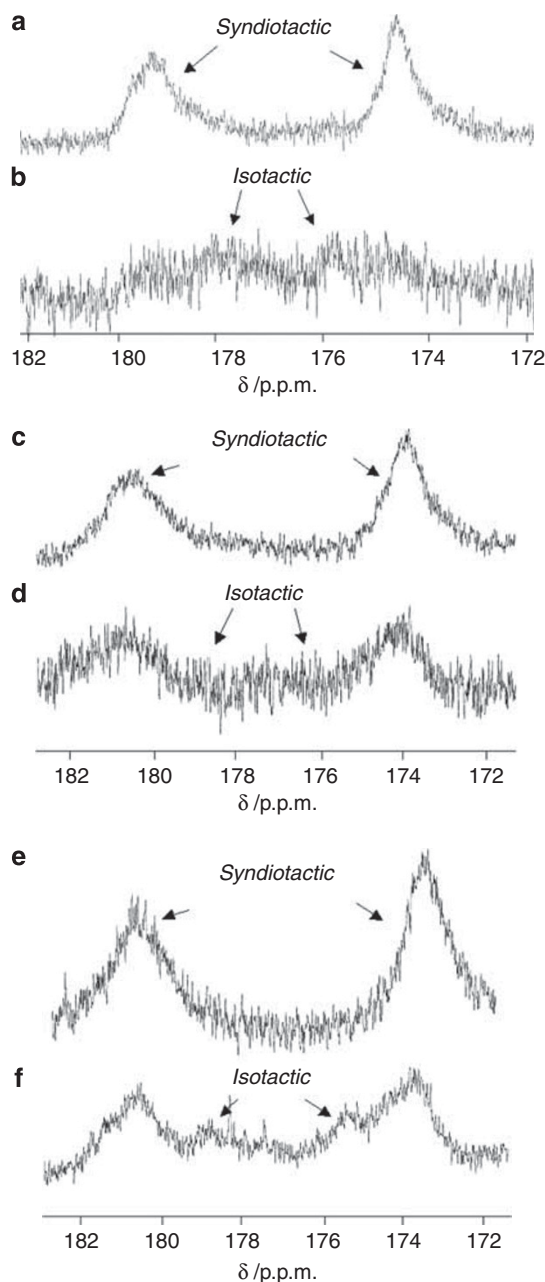


Figure 6 ^{13}C NMR spectra of poly(MRII) obtained by the anionic and radical method: (a) poly[(*R*)-MPGII] obtained with AIBN in Tol. at 60°C ($[\alpha]_{435} = -18.0^\circ$), (b) poly[(*S*)-MPGII] obtained with *n*-BuLi/(*S,S*)-Bnbox in Tol. at -40°C ($[\alpha]_{435} = -38.5^\circ$), (c) poly[(*S*)-MPAII] obtained with AIBN in Tol. at 60°C ($[\alpha]_{435} = -202.2^\circ$), (d) poly[(*S*)-MPAII] obtained with *n*-BuLi/(*S,S*)-Bnbox in Tol. at 0°C ($[\alpha]_{435} = -185.3^\circ$), (e) poly[(*S*)-MLII] obtained with AIBN in Tol. at 60°C ($[\alpha]_{435} = -128.8^\circ$) and (f) poly[(*S*)-MLII] obtained with *n*-BuLi/(–)-Sp in Tol. at 0°C ($[\alpha]_{435} = -69.1^\circ$).

Structures of Poly(MRII)s

To clarify the structure of poly(MRII), the ^{13}C NMR spectra were measured for the polymers obtained with several initiators. Figure 6 displays the partial ^{13}C NMR spectra of poly[(*S*)-MPGII] and poly[(*R*)-MPGII] (Figure 6a; run 9 in Table 1, and Figure 6b; run 2 in Table 2), poly[(*S*)-MPAII] (Figure 6c; run 9 in Table 3, and Figure 6d; run 6 in Table 3) and poly[(*S*)-MLII] (Figure 6e; run 13 in Table 4, and Figure 6f; run 2 in Table 4) obtained by asymmetric anionic polymerizations and radical polymerizations.

In general, poly(RII)s with a *syndiotactic* structure showed two broad peaks (173–175 and 179–182 p.p.m.) assigned to carbonyl groups in an imide ring, according to the ^{13}C NMR spectra for poly(*n*-butylitaconimide) and poly(*n*-diphenylmethylitaconimide). In contrast, poly(RII)s with an *isotactic* structure exhibited new peaks at about 175 and 178 p.p.m., which could be assigned to carbonyl carbons in the imide ring.^{24,25}

For the radical polymerizations of MLII, the resulting polymer showed two broad peaks due to the syndiotactic structure (Figure 6e; run 13 in Table 4). In contrast, for the anionic polymerization, the resulting poly(MLII) clearly showed two broader peaks due to the syndiotactic structure and two broader peaks due to the isotactic structure, all four of which were very small (Figure 6e; run 13 in Table 4, and Figure 6f; run 2 in Table 4). Consequently, poly(MLII)s obtained by the anionic polymerization are both *isotactic* and *syndiotactic*, meaning a partial form of helical conformation. However, the tacticity of poly(MRII)s has not yet been quantified because of the poor resolution of the peaks.

CONCLUSIONS

Asymmetric anionic polymerizations of chiral MRIIs, such as (*S*)-MPGII, (*R*)-MPGII, (*S*)-MPAII and (*S*)-MLII, were conducted with organometal–chiral ligand complexes to obtain optically active polymers. The yields, M_n s and the chiroptical properties of poly(MRII)s were strongly affected by the organometals, ligands, solvents and temperature. In addition, the behaviors of poly(MRII)s were different according to *N*-substituents.

The chirality of the polymers was attributable not only to the chirality of the optically active amino-acid units but also to the conformational chirality of the polymer main chain induced by the anionic polymerizations, according to the results of CD, ^{13}C NMR spectra and GPC curves obtained with polarimetric and UV detectors. In addition, the polymers obtained with *n*-BuLi/ligand complexes as anionic initiators showed higher stereoregularity than those obtained with a radical initiator.

In the ^{13}C NMR measurement, the spectrum of poly[(*S*)-MLII] obtained by the anionic polymerization showed new small peaks due to an *isotactic* structure, which differed from the spectrum of radical polymerization, which means that the poly[(*S*)-MLII] obtained by the anionic polymerization might partially form helical conformations.

More detailed polymerization abilities, chiroptical properties and higher-order structures of poly(RII) with various *N*-substituent groups are currently under investigation.

CONFLICT OF INTEREST

The authors declare no conflict of interest.

- Okamoto, Y. & Nakano, T. Asymmetric polymerization. *Chem. Rev.* **94**, 349–372 (1994).
- Nakano, T. & Okamoto, Y. Synthetic helical polymers: conformation and function. *Chem. Rev.* **101**, 4013–4038 (2001).

- Azam, A., Fakhrol, K. M., Kamigaito, M. & Okamoto, Y. Asymmetric radical polymerization and copolymerization of *N*-(1-phenyldibenzosuberyl)methacrylamide and its derivative leading to optically active helical polymers. *J. Polym. Sci., Part A, Polym. Chem.* **45**, 1304–1315 (2007).
- Nomura, R., Fukushima, Y., Nakako, H. & Masuda, T. Conformational study of helical poly(propionic esters) in solution. *J. Am. Chem. Soc.* **122**, 8830–8836 (2000).
- Aoki, T., Kaneko, T., Maruyama, N., Sumi, A., Takahashi, M., Sato, T. & Teraguchi, M. Helix-sense-selective polymerization of phenylacetylene having two hydroxy groups using a chiral catalytic system. *J. Am. Chem. Soc.* **125**, 6346–6347 (2003).
- Yashima, E., Maeda, K. & Nishimura, T. Detection and amplification of chirality by helical polymers. *Chem. Eur. J.* **10**, 42–51 (2004).
- Lee, H. J., Jin, Z. X., Aleshin, A. N., Lee, J. Y., Goh, M. J., Akagi, K., Kim, Y. S., Kim, D. W. & Park, Y. W. Dispersion and current-voltage characteristics of helical polyacetylene single fibers. *J. Am. Chem. Soc.* **126**, 16722–16723 (2004).
- Green, M. M., Park, J. W., Sato, T., Teramoto, A., Lifson, S., Selinger, R. L. B. & Selinger, J. V. The macromolecular route to chiral amplification. *Angew. Chem. Int. Ed.* **38**, 3139–3154 (1999).
- Kamer, P. C. J., Nolte, R. J. M. & Drenth, W. Screw sense selective polymerization of achiral isocyanides catalyzed by optically active nickel(II) complexes. *J. Am. Chem. Soc.* **110**, 6818–6825 (1988).
- Deming, T. J. & Novak, B. M. Mechanistic studies on the nickel-catalyzed polymerization of isocyanides. *J. Am. Chem. Soc.* **115**, 9101–9111 (1993).
- Onitsuka, K., Yabe, K., Ohshiro, N., Shimizu, A., Okumura, R., Takei, F. & Takahashi, S. Di- and trifunctional initiators containing pt-pd μ -ethynediyl units for living polymerization of aryl isocyanides. *Macromolecules* **37**, 8204–8211 (2004).
- Tabei, J., Nomura, R. & Masuda, T. Conformational study of Poly(*N*-propargylamides) having bulky pendant groups. *Macromolecules* **35**, 5405–5409 (2002).
- Gao, G., Sanda, F. & Masuda, T. Synthesis and properties of amino acid-based polyacetylenes. *Macromolecules* **36**, 3932–3937 (2003).
- Zhao, H., Sanda, F. & Masuda, T. Chemistry and physics control of helical sense and tightness of amino acid-based poly(*N*-propargylamide) by temperature and solvents. *Macromolecular* **206**, 1653–1658 (2005).
- Liu, R., Sanda, F. & Masuda, T. Polymer synthesis and properties of ornithine- and lysine-based poly(*N*-propargylamides). Responsiveness of the helical structure to acids. *Polymer* **48**, 6510–6518 (2007).
- Oishi, T., Onimura, K., Tanaka, K. & Tsutsumi, H. Asymmetric polymerization of *N*-substituted maleimides with chiral oxazolidine-organolithium. *J. Polym. Sci., Part A: Polym. Chem.* **37**, 473–482 (1999).
- Zhou, H., Onimura, K., Tsutsumi, H. & Oishi, T. Asymmetric anionic polymerization of chiral (*R*)-(+)-*N*- α -methylbenzylmaleimide with chiral ligand/organometal complex. *Polym. J.* **32**, 552–559 (2000).
- Isobe, Y., Onimura, K., Tsutsumi, H. & Oishi, T. Asymmetric anionic polymerization of *N*-1-naphthylmaleimide with chiral ligand-organometal complexes in toluene. *J. Polym. Sci., Part A: Polym. Chem.* **39**, 3556–3565 (2001).
- Zhou, H., Onimura, K., Tsutsumi, H. & Oishi, T. Synthesis and chiroptical properties of (*S*)-(-)-*N*- α -methylbenzylmaleimide polymers containing crystallinity. *Polym. J.* **33**, 227–235 (2001).
- Isobe, Y., Onimura, K., Tsutsumi, H. & Oishi, T. Asymmetric polymerization of *N*-1-anthrylmaleimide with diethylzinc-chiral ligand complexes and optical resolution using the polymer. *Polym. J.* **34**, 18–24 (2002).
- Zhang, Y., Onimura, K., Tsutsumi, H. & Oishi, T. Asymmetric anionic polymerization of (*S*)-(-)-*N*-maleoyl-L-valine methyl ester. *Polym. J.* **36**, 878–887 (2004).
- Oishi, T., Zhang, Y., Fukushima, T. & Onimura, K. Asymmetric anionic polymerizations of (*R*)-*N*-maleoyl-D-phenylglycine alkyl esters and optical resolution using their polymers. *Polym. J.* **37**, 453–463 (2005).
- Gao, H., Isobe, Y., Onimura, K. & Oishi, T. Asymmetric polymerization of (*S*)-*N*-maleoyl-L-leucine allyl ester and chiral recognition ability of its polymer as chiral stationary phase for HPLC. *Polym. J.* **39**, 764–776 (2007).
- Matsumoto, A., Umehara, S., Watanabe, H. & Otsu, T. Poly(*N*-*n*-butylitaconimide). Preparation and characterization. *J. Polym. Sci., Polym. Phys.* **31**, 527–535 (1993).
- Watanabe, H., Matsumoto, A. & Otsu, T. Polymerization of *N*-alkyl-substituted itaconimides and *N*-(alkyl-substituted phenyl)itaconimides and characterization of the resulting polymers. *J. Polym. Sci., Part A, Polym. Chem.* **32**, 2073–2083 (1994).
- Oishi, T. & Kawamoto, T. Synthesis and polymerization of optically active *N*-[4-*N*-(α -methylbenzyl)aminocarbonylphenyl]itaconimide. *Polym. J.* **26**, 920–929 (1994).
- Oishi, T., Nagai, K., Kawamoto, T. & Tsutsumi, H. Synthesis and polymerization of *N*-[4-(cholesteroxycarbonyl)phenyl]itaconimide. *Polymer* **37**, 3131–3139 (1996).
- Oishi, T., Onimura, K., Sumida, W., Kobayashi, T. & Tsutsumi, H. Asymmetric anionic polymerization of *n*-diphenylmethylitaconimide with chiral ligand-organometal complex. *Polym. Bull.* **48**, 317–325 (2002).
- Gao, H., Isobe, Y., Onimura, K. & Oishi, T. Asymmetric polymerizations of *N*-substituted maleimides bearing L-leucine ester derivatives and chiral recognition abilities of their polymers. *Polym. J.* **39**, 1047–1059 (2007).
- Ueda, M., Mano, M., Mori, H. & Ito, H. Polymerization of α -methyleneindane: a cyclic analog of α -methylstyrene. *J. Polym. Sci., Part A: Polym. Chem.* **29**, 1779–1787 (1991).
- Suenaga, J., Sutherland, D. M. & Stille, J. K. Polymerization of (*RS*-) and (*R*)- α -methylene- γ -methyl- γ -butyrolactone. *Macromolecules* **17**, 2913–2916 (1984).
- Miyagawa, T., Sanda, F. & Endo, T. Synthesis and radical polymerization of 5-methylene-2,2-dimethyl-1,3-dioxolan-4-one. *J. Polym. Sci., Part A: Polym. Chem.* **38**, 1861–1865 (2000).

- 33 Kawauchi, T., Nakamura, M., Kitayama, T., Padias, B. & Hall, H. K. Jr. Structural analyses of methyl bicyclobutane-1-carboxylate oligomers formed with tert-butyl-lithium/aluminum bisphenoxide and mechanistic aspect of the polymerization. *Polym. J.* **37**, 439–448 (2005).
- 34 Nakano, T., Takewaki, K., Yade, T. & Okamoto, Y. Dibenzofulvene, a 1,1-diphenyl-ethylene analogue, gives a δ -stacked polymer by anionic, free-radical, and cationic catalysts. *J. Am. Chem. Soc.* **123**, 9182–9183 (2001).
- 35 Nakano, T. & Yade, T. Synthesis, structure, and photophysical and electrochemical properties of a δ -stacked polymer. *J. Am. Chem. Soc.* **125**, 15474–15484 (2003).
- 36 Nakano, T., Nakagawa, O., Tsuji, M., Tanikawa, M., Yade, T. & Okamoto, Y. Poly(2,7-dipentylidibenzofulvene) showing chiroptical properties in the solid state based purely on a chiral conformation. *Chem. Commun.* 144–145 (2004).
- 37 Nakano, T. Synthesis, structure and function of π -stacked polymers. *Polym. J.* **42**, 103–123 (2010).